Journal of Non-Newtonian Fluid Mechanics, 35 (1990) 287–307
Elsevier Science Publishers B.V., Amsterdam – Printed in The Netherlands

CLIMBING CONSTANT, SECOND-ORDER CORRECTION OF TROUTON'S VISCOSITY, WAVE SPEED AND DELAYED DIE SWELL FOR M1

HOWARD H. HU, OLIVER RICCIUS, KANG PING CHEN, MIKE ARNEY and DANIEL D. JOSEPH

Department of Aerospace Engineering and Mechanics, University of Minnesota, 107 Akerman Hall, Minneapolis, MN 55455 (U.S.A.)

(Received April 1, 1989; in revised form August 2, 1989)

Abstract

Measurements of the wave speed c in M1 imply a fast time $\lambda = \mu/\rho c^2$ of relaxation. This and the delayed die-swell measurements suggest that M1 is not very elastic. Extensive and very reliable values of the climbing constants show that M1 has weak normal stresses at the level of STP. The climbing constants plus back-extrapolated values of $N_1/\dot{\gamma}^2$ taken from measurements at two temperatures by Binding, and Walters and Prud'homme lead to values of the two coefficients in the second-order regime of slow flow of M1. This gives us all the constants in the Roscoe formula for the quadratic correction of Trouton's viscosity and also allows us to compute the normal stress ratio $-N_2/N_1 \doteq 0.11$, independent of temperature.

Keywords: climbing constant; delayed die swell; extensional viscosity; wave speed; test fluid M1

1. Introduction

The rheometrical data presented in this report are unique in that it is the only report on the properties of the M1 fluid to present measured values of the climbing constant, of the two constants of the second-order approximation of a viscoelastic fluid, of the intensity factor for extensional viscosity, and secondary motions at second order. We computed $N_2/N_1 = -0.11$ at low shears from our measured climbing constant at 20 °C and back extrapolation of $N_1/2\dot{\gamma}^2$ given by K. Walters. We computed $N_2/N_1 = -0.12$ at low shears from our measured climbing constant at 27.2 °C and back extrapolation of $N_1/2\dot{\gamma}^2$ as given by R.K. Prud'homme. We are also the only

laboratory to give values of the wave speed, the rigidity and the effective time of relaxation. Our time of relaxation is shorter than that computed in the traditional way using standard rheometers. The reason for this is that the response time of the wave speed meter is much shorter (say 10^{-4}–10^{-3} s) than the response time of cone-and-plate rheometers (10^{-1} s). The speeds which we measure and the associated relaxation times seems to correlate with various critical phenomena which occur in the flow of polymeric liquids, the most notable being delayed die swell. We present some data for delayed die swell in the M1 solution. The M1 solution has a fast time of relaxation as is characteristic of fluids with a rather more Newtonian than elastic response.

2. Theory

The operational theory for the measurement of the climbing constant is given in the 1984 paper of Joseph et al. [1]. The height function for the climb is given by

$$H(r, \Omega) = h_0(r) + h_2(r)\Omega^2, \tag{2.1}$$

where Ω is the angular frequency and terms of $O(\Omega^4)$ have been neglected. Here $h_0(r)$ is the static climb, independent of Ω, and $h_2(r)$ is to be determined by the following problem:

$$\frac{T}{r}(rh_2')' - \rho g h_2 = -2\frac{a^4}{r^4}\hat{\beta} + \frac{\rho a^4}{2r^2}, \tag{2.2}$$
$$h_2'(a) = 0,\ h_2(r) \to 0 \text{ as } r \to \infty$$

where T is the surface tension,

$$\hat{\beta} = 3\alpha_1 + 2\alpha_2 \tag{2.3}$$

is the climbing constant, α_1 and α_2 are constants of the quadratic approximation to $\boldsymbol{S}$ in the stress $\boldsymbol{T} = p\boldsymbol{1} + \boldsymbol{S}$, $\boldsymbol{S} = \boldsymbol{S}_1 + \boldsymbol{S}_2 \ldots$,

$\boldsymbol{S}_1 = \mu \boldsymbol{A}_1[\boldsymbol{U}]$ is the linear or Newtonian approximation,

$$\boldsymbol{S}_2 = \alpha_1 \boldsymbol{A}_2[\boldsymbol{U}] + \alpha_2 \boldsymbol{A}_1^2[\boldsymbol{U}]. \tag{2.4}$$

The expression $\boldsymbol{S}_{(2)} = \boldsymbol{S}_1 + \boldsymbol{S}_2$ is called the extra stress of a fluid of grade two. This is just a way of speaking; there is no fluid of grade two, but such an expression arises on every simple fluid when the flow is slow and slowly varying; for a recent full discussion see Joseph [2]. The constants α_1 and α_2 are related to the zero shear values of the first and second normal stress differences N_1 and N_2 by the following:

$$\begin{aligned} T_{11} - T_{22} &= N_1 = -2\alpha_1 \dot{\gamma}^2, \\ T_{22} - T_{33} &= N_2 = (2\alpha_1 + \alpha_2)\dot{\gamma}^2, \end{aligned} \tag{2.5}$$

where $\dot{\gamma}$ is the shear rate and

$$T_{12} = \dot{\gamma}\mu. \tag{2.6}$$

If we define

$$\begin{aligned} n_1 &= \lim_{\dot{\gamma}\to 0} N_1/\dot{\gamma}^2, \\ n_2 &= \lim_{\dot{\gamma}\to 0} N_2/\dot{\gamma}^2, \end{aligned} \tag{2.7}$$

then

$$\begin{aligned} \alpha_1 &= -n_1/2, \\ \alpha_2 &= n_1 + n_2, \\ \hat{\beta} &= 3\alpha_1 + 2\alpha_2 = \frac{n_1}{2} + 2n_2. \end{aligned} \tag{2.8}$$

The fluid will not climb a rod if $n_2/n_1 < -1/4$. The theory of rod climbing with surface tension neglected was done by Kaye [3], Joseph and Fosdick [4], Hoffman and Gottenberg [5], and Böhme [6]. Joseph et al. [7] were the first to use theory in experiments designed to measure $\hat{\beta}$. They showed that, to get the predicted shapes of the free surface to agree with measured ones, it is necessary to retain the effects of surface tension, as in (2.2). A very accurate approximate solution of (2.2) was derived by Joseph et al. [7]. When evaluated at the rod this solution gives

$$h_2(a) \sim \frac{a}{2T\sqrt{S}}\left(\frac{4\hat{\beta}}{4+\lambda} - \frac{\rho a^2}{2+\lambda}\right), \tag{2.9}$$

where $\lambda^2 = a^2 S$ and $S = \rho g/T$. Joseph et al. [7] and Beavers and Joseph [8] proposed (2.2) and (2.9) as a basis for a rotating rod viscometer. A possible defect of this kind of rheometer is that it requires values for the surface tension. Fortunately, the values of T which have been measured in the different liquids used in experiments and in M1 are nearly the same, about 30×10^{-5} N cm^{-1}. An error analysis given by Joseph et al. [1] shows that the value computed for $\hat{\beta}$ from the graph of the measured height of climb at the rod is not strongly affected by small changes in surface tension.

Roscoe [9] presented a formula for the extensional viscosity at low rates of shearing

$$T_{11} - T_{22} = 3\left[\dot{s}\mu + (\alpha_1 + \alpha_2)\dot{s}^2\right] + O(|\dot{s}|^3), \tag{2.10}$$

where $\dot{s}$ is the rate of stretching. This is probably the only model-independent formula for extensional viscosity which can be evaluated numerically by relatively simple rheological measurements. Equation (2.10) was given, in a slightly different form, by Zahorski [10].

Using (2.8), we find that

$$\alpha_1 + \alpha_2 = \frac{n_1}{2} + n_2. \tag{2.11}$$

Fluids with $n_2/n_1 < -1/2$ stretch weaken. Equation $(2.8)_3$ shows that such a fluid will not climb a rod. We also note that

$$\begin{aligned} \alpha_1 &= 2n_2 - \hat{\beta}, \\ \alpha_2 &= 2\hat{\beta} - 3n_2, \\ \alpha_1 + \alpha_2 &= \hat{\beta} - n_2. \end{aligned} \tag{2.12}$$

Equation $(2.12)_3$ shows that the intensity factor for extensional flow, the second-order correction of the Trouton viscosity, is equal to the climbing constant when $n_2 = 0$. It is easily verified that $\alpha_1 + \alpha_2 = \frac{4}{3}\hat{\beta}$ when $n_2/n_1 = -1/10$.

Joseph [2] has shown that the intensity factor $\alpha_1 + \alpha_2$ for the extensional viscosity at second order also controls the creation of vortices at second order in the following sense: suppose that the vorticity $\zeta = \epsilon\zeta_1 + \epsilon^2\zeta_2 + O(\epsilon^3)$, where ϵ is a parameter perturbing rest. Then we find that ζ_1 and ζ_2 satisfy

$$\nabla^2\zeta_1 = \mathbf{0} \tag{2.13}$$

and

$$\rho\frac{\partial\zeta_2}{\partial t} + \rho\ \mathrm{curl}(\zeta_1 \wedge \boldsymbol{u}_1) = \mu\nabla^2\zeta_2 + (\alpha_1 + \alpha_2)\mathrm{curl\ div}\, A_1^2. \tag{2.14}$$

Equations (2.13) and (2.14) show that the effects of viscoelasticity on the vorticity appear first at second order with an intensity factor $\alpha_1 + \alpha_2$.

How should the constants α_1 and α_2 be measured? The climbing constant (2.3) gives one combination of α_1 and α_2 which can be measured with very good precision. The hard-to-measure second normal stress is related to α_1 and α_2 by

$$n_2 = 2\alpha_1 + \alpha_2. \tag{2.15}$$

It is claimed that n_2 can be measured by measuring the surface deflection in a tilted trough. A full discussion of this method is given by Tanner [11]. The shear rates which can be achieved in a trough tilted through a small angle are rather small so that the deflections which develop on the free surface would not be easy to measure in many fluids. The comparison of Table 2 and Table 3 giving $\alpha_1 + \alpha_2$ for the fluids D1 and M1 suggests that the surface deflections in M1 would be more than 50 times smaller than in D1. In fact, rheological data using this method are rather sparse.

The second normal stress can be obtained in measurements on ordinary cone-and-plate rheometers by a well-known method. The problem with this

method is that the values of the first and second normal stresses at low shearing cannot usually be obtained because the transducers will not work unless the shear is above a certain threshold. However, it is very easy to show [2] that, at low rates of shearing, the ratio of the normal stress differences has a limiting value

$$-\frac{N_2}{N_1} = 1 + \frac{\alpha_2}{2\alpha_1} + O(\dot{\gamma}^2), \tag{2.16}$$

with

$$-\frac{n_2}{n_1} = 1 + \frac{\alpha_2}{2\alpha_1}. \tag{2.17}$$

Hence, we may hope that (2.15) may be measured by backward extrapolation of the values of $-N_2/N_1$ measured on cone-and-plate rheometers. The values of α_1 and α_2 may now be determined:

$$\alpha_1 = -\frac{1}{1 + 4n_2/n_1}\hat{\beta}, \tag{2.18}$$

$$\alpha_2 = 2\frac{1 + n_2/n_1}{1 + 4n_2/n_1}\hat{\beta}, \tag{2.19}$$

$$\alpha_1 + \alpha_2 = \frac{1 + 2n_2/n_1}{1 + 4n_2/n_1}\hat{\beta}. \tag{2.20}$$

Evidently $N_2/2\dot{\gamma}^2$ is too small to measure in M1 so that back extrapolation of N_2/N_1 without considerable scatter cannot be carried out. However, it seems that the graphs of $N_1/2\dot{\gamma}^2$ shown in Figs. 8 and 9 can be extrapolated to give $-\alpha_1$. Then α_1 and $\hat{\beta}$ determine α_2 and N_2/N_1 uniquely.

3. Climbing constants

The climbing constants (Fig. 1) were measured using a rotating rod viscometer. We have figures like those of Figs. 2–5 for every one of the 38

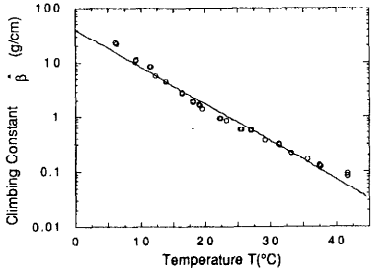

Fig. 1. Summary of the dependence of climbing constant $\hat{\beta}$ on temperature T (6.2–41.5 °C). The equation of the line is $\hat{\beta} = 39.7\exp(-0.158T)$ g cm^{-1}. At $T = 20$ °C, $\hat{\beta} = 1.68$ g cm^{-1}.

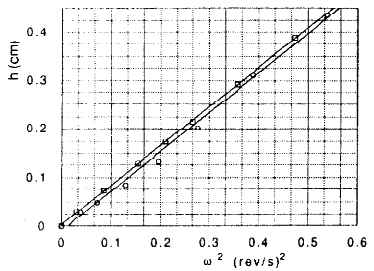

Fig. 2. Height rise h (cm) at the rod vs. the angular velocity squared ω^2 ((rev $s^{-1})^2$). ○ (angular velocity increases), $h = -0.011 + 0.817\omega^2$; □ (angular velocity decreases), $h = 1.8 \times 10^{-3} + 0.813\omega^2$. The average climbing constant is $\hat{\beta} = 23.2$ g cm^{-1} at $T = 6.2°$ C.

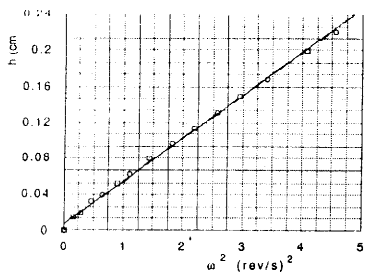

Fig. 3. Height rise h (cm) at the rod vs. the angular velocity squared ω^2 ((rev $s^{-1})^2$). ○ (angular velocity increases), $h = 6.65 \times 10^{-3} + 0.0478\omega^2$; □ (angular velocity decreases), $h = 6.99 \times 10^{-3} + 0.0479\omega^2$. The average climbing constant is $\hat{\beta} = 1.43$ g cm^{-1} at $T = 19.45°$ C.

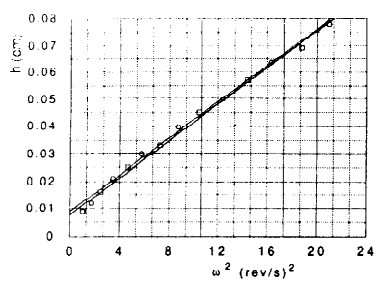

Fig. 4. Height rise h (cm) at the rod vs. the angular velocity squared ω^2 ((rev $s^{-1})^2$). ○ (angular velocity increases), $h = 9.00 \times 10^{-3} + 0.00335\omega^2$; □ (angular velocity decreases), $h = 7.70 \times 10^{-3} + 0.00338\omega^2$. The average climbing constant is $\hat{\beta} = 0.168$ g cm^{-1} at $T = 35.55°$ C.

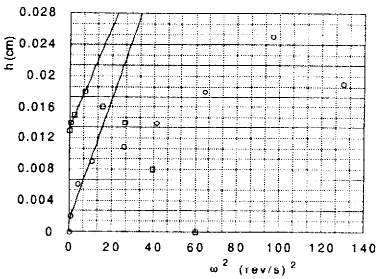

Fig. 5. Height rise h (cm) at the rod vs. the angular velocity squared ω^2 ((rev $s^{-1})^2$). ○ (angular velocity increases), for the first four points $h = 1.19 \times 10^{-3} + 7.90 \times 10^{-4}\omega^2$; □ (angular velocity decreases), for the first four points $h = 0.0133 + 6.53 \times 10^{-4}\omega^2$. At this temperature, the fluid sinks for higher values of angular velocity. The average climbing constant is $\hat{\beta} = 0.093$ g cm^{-1} at $T = 41.5°$ C.

entries in Table 1. In Table 1 we also list the test date as a check to see whether the M1 is time dependent or not. As indicated in the table M1 is not time dependent, at least for a period of time.

Surface tension of the fluid $T = 29.9 \times 10^{-5}$ N cm^{-1}, density of the fluid $\rho = 0.895$ g cm^{-3} and the radius of the steel rod $a = 0.474$ cm. T and ρ are almost constant for the temperature range of our measurements. The surface tension was measured with a ring tensiometer.

The diameter of the fluid container, which is made of copper, is 10 cm. The angular speed of the rod can be measured to within 0.002 rev s^{-1}. The measurements of the height of climb are repeatable to within 0.002 cm. The rod and fluid are enclosed in a Plexiglas chamber which is connected to a temperature controller. The temperature is measured at the surface of the fluid and the probe is kept at the same position for all the measurements. There are temperature differences between the fluid and air in the chamber; for more accurate measurement we need a better way to control the temperature.

At larger rotational speeds the steady climbing bubble loses stability to a time-dependent motion which has been called the "breathing instability". This motion first appears at a critical $\omega = \omega_c$, then grows quickly to time-periodic motion with a long period in which a band on fluid rises slowly to a certain height, then collapses down into the body of fluid. The time-periodic breathing motion in M1 is shown in Figs. 6(c)–6(f) and in photographs displayed in Figs. 95.2 and 95.3 by Joseph [12]. A general description of the breathing instability is in the reference just mentioned, in Beavers and Joseph [8], and in Joseph and Beavers [13].

The first quantitative data for the breathing instability are presented in Fig. 7 where the critical speed is plotted against the temperature and fit to

TABLE 1

Measured values of climbing constants. All data was taken in February 1989. M1 is not time dependent at least for a period of time

Temperature (°C)	Climbing constant $\hat{\beta}$ (g cm^{-1})	Date
6.2	23.2	14
6.3	21.8	14
9.15	11.3	15
9.15	11.5	15
12.25	5.80	15
12.3	5.76	15
16.3	2.80	16
16.3	2.87	16
18.9	1.67	16
18.95	1.59	16
22.1	0.931	16
22.2	0.934	16
25.4	0.568	17
25.3	0.585	17
29.05	0.366	18
28.95	0.379	18
32.9	0.219	18
32.95	0.217	18
37.25	0.130	19
37.35	0.128	19
41.5	0.083	20
41.5	0.093	20
35.5	0.173	20
35.55	0.168	20
31.15	0.304	21
31.15	0.317	21
26.9	0.576	21
26.95	0.564	21
23.15	0.876	21
23.1	0.873	21
19.45	1.43	22
19.45	1.43	22
18	1.97	22
17.95	1.88	22
13.9	4.61	23
13.8	4.53	23
11.45	8.49	23
11.35	8.75	23

the curve $\omega_c = \exp(0.074T)$. Recalling now that $\hat{\beta} = 39.7 \exp(-0.158T)$ we may conclude that the critical speed ω_c is proportional to $1/\sqrt{\hat{\beta}}$, approximately.

4. Limiting values of the normal stresses

Thrust measurements on the plate of a cone-and-plate rheometer give the normal stress difference $N_1(\dot{\gamma})$ as a function of the shear rate $\dot{\gamma}$. The same thrust measurements in a parallel plate rheometer give values of $N_2 - N_1$ where $N_2(\dot{\gamma})$ is the second normal stress difference. Neither measurement can be easily carried to low rates of shear because of the insensitivity of the

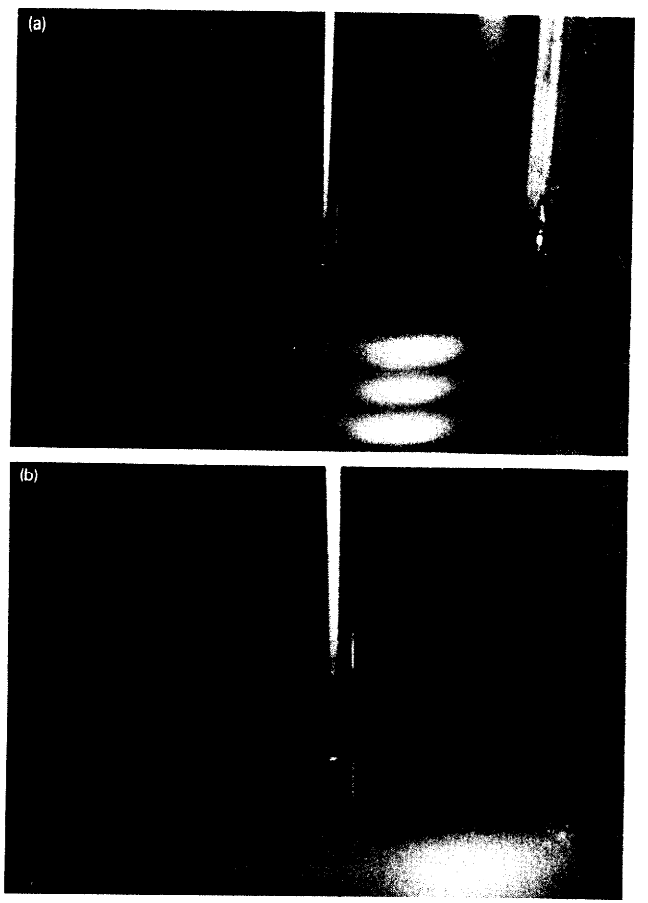

Fig. 6(a–f). Photographs of rod climbing in M1 at 21.5°C. (a) At rest, there is a small static climb due to capillarity; (b) stable steady climb $\omega = 3$ rev s^{-1}; (c) and (d), slightly post critical time-periodic motion at $\omega = 4.94$ rev s^{-1}; (e) and (f), large amplitude time-periodic motion at $\omega = 6.55$ rev s^{-1}.

transducer. From these two measurements, we can compute N_2/N_1 as a function of $\dot{\gamma}$ and try to extrapolate it to zero shear. This first procedure works well for the test fluid D1 used in the second normal stress difference project [14]. From Fig. 5 of Ref. 14 we easily estimate by extrapolation to zero shear

$$0.07 \leq -\frac{N_2}{N_1} \leq 0.10 \text{ at } 25\,^{\circ}\text{C}. \tag{4.1}$$

The climbing constant for D1 at 25°C was measured by us as

$$\hat{\beta} = 62.2\,\text{g cm}^{-1}. \tag{4.2}$$

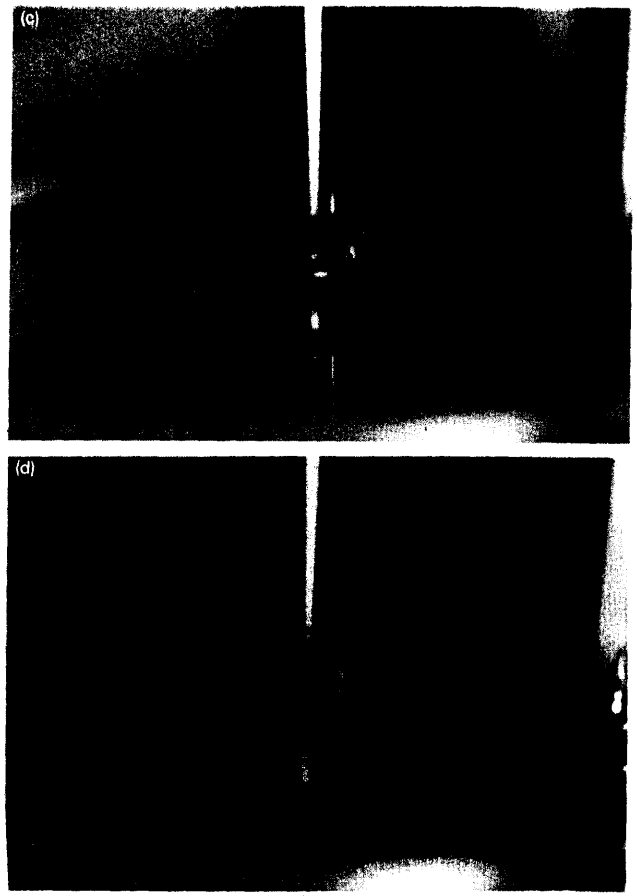

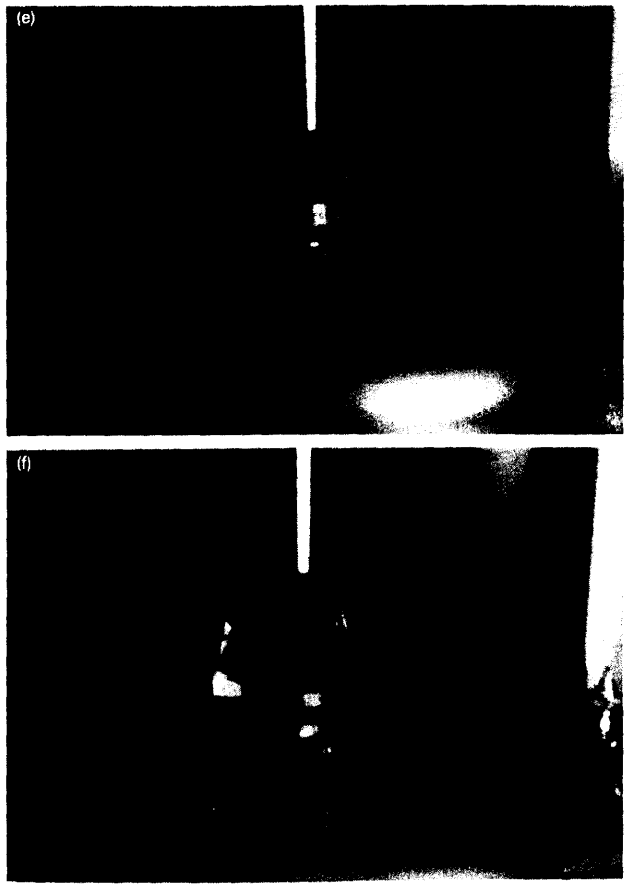

In Table 2 we have given the values of the quadratic constants α_1 and α_2 computed from (4.1) and (4.2) using (2.8) and (2.17) and the values of the limiting normal stress n_1 and n_2 using α_1 and α_2 in (2.5) and (2.7).

The normal stresses in M1 are more than 50 times smaller than in D1. However, it appears to be possible to back extrapolate $N_1/2\dot{\gamma}^2$ to its limiting value $-\alpha_1$. This, together with the climbing constant $\hat{\beta} = 3\alpha_1 + 2\alpha_2$, gives α_1 and α_2 separately. Figure 8 gives measured values of $N_1/2\dot{\gamma}^2$ for M1 at 20°C which were measured in Professor Walters' laboratory on a Weissenberg rheogoniometer. Figure 9 gives measured values of $N_1/2\dot{\gamma}^2$ for M1 at 27.2°C which were measured on a System IV Rheometrics rheometer

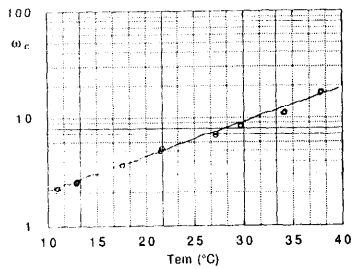

Fig. 7. Dependence of the critical speed of instability ω_c on temperature (°C). The equation of the line is $\omega_c = \exp(0.074T)$ rev s^{-1}.

TABLE 2

Material parameters for D1 at 25°C using (4.1) and (4.2)

	$-n_2/n_1 = 0.10$	$-n_2/n_1 = 0.07$
$\hat{\beta}$ (g cm^{-1})	62.2	62.2
α_1 (g cm^{-1})	−103	−86
α_2 (g cm^{-1})	187	161
$\alpha_1 + \alpha_2$	84	75
n_1 (g cm^{-1})	206	172
n_2 (g cm^{-1})	−17	−11

with a sensitive transducer in the laboratory of R.K. Prud'homme. From the extrapolated values $\alpha_1 = -3.0$ g cm^{-1} at 20°C and $\alpha_1 = -1.0$ g cm^{-1} at 27.2°C and the values $\hat{\beta} = 1.68$ g cm^{-1} at 20°C and $\hat{\beta} = 0.54$ g cm^{-1} taken from Fig. 1, we compute the entries in Table 3.

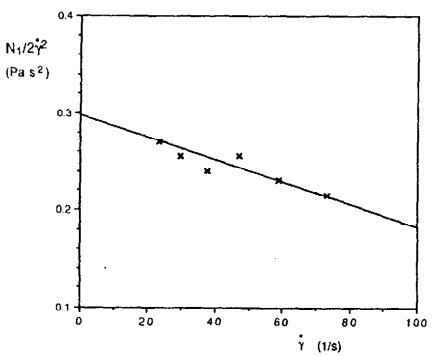

Fig. 8. Measured values of $N_1/2\dot{\gamma}^2$ for M1 at 20°C. The backward extrapolation gives that $N_1/2\dot{\gamma}^2 \to -\alpha_1$ is about 0.3 Pa s^2 or 3 g cm^{-1}. (After Binding et al. [15].)

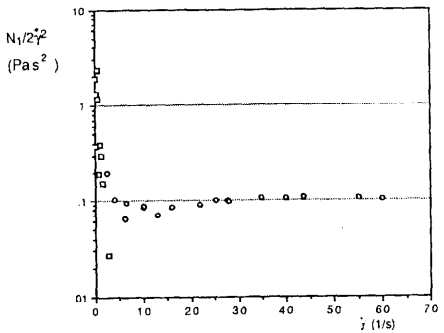

Fig. 9. Measured values of $N_1/2\dot{\gamma}^2$ for M1 at 27.2°C. The measured values of the stress for □ are below the allowed transducer limits and are discarded. We took the limiting value to be $-\alpha_1 = 0.1$ Pa s^2 or 1 g cm^{-1}. (After Prud'homme [16].)

Table 3 shows that N_2/N_1 is very insensitive to changes in the temperature even over a range of temperature in which the values N_1 and N_2 depend strongly on the temperature. The value of N_2/N_1 is also not very sensitive to errors in the measurement of $n_1 = -2\alpha_1$. At the Combloux meeting measurements at 20°C were reported in the range

$$2.77 \text{ g cm}^{-1} \leq -\alpha_1 \leq 3.50 \text{ g cm}^{-1}.$$

Using $\hat{\beta} = 1.68$ we compute

$$0.097 \leq -N_2/N_1 \leq 0.129.$$

This range of values is consistent with N_2/N_1 data presented by Binding et al. [15].

TABLE 3

Material parameters for M1 at 20°C and 27.2°C using (4.1) and (4.2)

	20°C	27.2°C
$-n_1/2 = \alpha_1$ (g cm^{-1})	−3.0	−1.0
$\hat{\beta}$ (g cm^{-1})	1.68	0.54
α_2 (g cm^{-1})	5.34	1.77
$\alpha_1 + \alpha_2$	2.34	0.77
N_2/N_1	−0.11	−0.12

5. Second-order correction of the Trouton viscosity

We turn next to an evaluation of the coefficients in the formula (2.10) which give the extensional viscosity

$$3[\mu + (\alpha_1 + \alpha_2)\dot{s}] \tag{5.1}$$

at low rates of stretching. Values for the coefficient $\alpha_1 + \alpha_2$ of the second-order correction of the Trouton viscosity are given in Tables 2 and 3. To complete the description of (5.1) we give values for the viscosity μ in Table 4. The elongational stress (2.10) for D1 at 25 °C when $n_2/n_1 = -0.10$ is

$$T_{11} - T_{22} \sim 3(95\dot{s} + 83.0\dot{s}^2). \tag{5.2}$$

Evaluation of the same stress for M1 at 20 °C gives

$$T_{11} - T_{22} \sim 3(29.5\dot{s} + 2.34\dot{s}^2). \tag{5.3}$$

At $T = 27.2$ °C we have

$$T_{11} - T_{22} \sim 3(11\dot{s} + 0.77\dot{s}^2). \tag{5.4}$$

Comparing now (5.2) and (5.3) we can conclude that the increase of

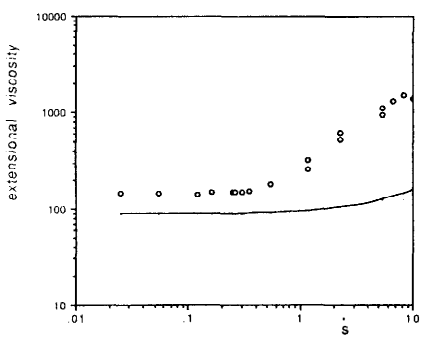

Fig. 10. Comparison of eqn. (5.3) with measurements at 20 °C of Mikkelsen et al. [7] using opposing jets.

TABLE 4

Values of the viscosity μ

Fluid	μ
D1 at 25 °C	9.5 Pa s
M1 at 20 °C	2.95 Pa s
M1 at 27.2 °C	1.1 Pa s

extensional viscosity at second order is more than 50 times greater in D1 than in M1.

In Fig. 10 we have compared measurements of Mikkelsen et al. [17], using Fuller's method of opposing jets, with our expression (5.3). It is known that the opposing jet gives a stretch value for the extensional viscosity which is about 1.4 times the Trouton viscosity. After taking into account the expected shift of 1.4 (see Schunk et al. [18]), we may conclude that the range of stretch rates for which second-order effects are negligible is the same for the exact formula (5.3). The nonlinear effects in the experiments undoubtedly extend beyond second order so that perhaps there is satisfactory agreement.

6. Wave speeds, effective rigidity and effective relaxation times

The shear-wave speed for M1 was measured with the wave-speed meter in our laboratory. The meter allows us to determine transit times for an impulsively generated shear wave in a fluid at rest. The wave traverses the gap between two concentric cylinders. Transit time measurements must be made for different gap sizes. We can vary the gap dimensions in our apparatus between 0.25 and 12.8 mm. A shear-wave speed is defined if we measure one and the same transit speed over a range of small gaps.

The theory for the wave-speed meter is given in Joseph et al. [19]. The apparatus and the measuring technique are described in Joseph et al. [20] and in detail in Riccius [21].

For the M1 fluid we measured transit times with three different gap sizes of 6.12, 9.38 and 12.2 mm. The transit speeds c presented in Table 5 are determined from averages over eight time measurements for each gap. The shear-wave speed $\bar{c}$ is then defined as the average over the three transit speeds. Examples of the raw data for each gap size are shown in Fig. 11. The raw data are voltage vs. time diagrams which are recorded on an oscilloscope. There are two signals for each gap size; each one is adjusted to 1.75 V before the measurement is started. The rapid drop of the first signal corresponds to the motion of the outer cylinder which is caused by the impacting kicking device. The second signal represents the motion of the

TABLE 5

Wave speed $\bar{c}$, effective rigidity G_c and effective relaxation time λ_c for M1

Gap (10^{-3} m)	c (cm s^{-1})	T (°C)	$\bar{c}$ (cm s^{-1})	G_c (Pa)	λ_c (10^{-3} s)	$\tilde{\mu}$ (Pa s)	ρ (kg m^{-3})
6.12	378.1 ± 12.1	23	404.7	14067	0.21	3.0	859
9.38	403.4 ± 33.6	23					
12.2	430.5 ± 10.5	23					

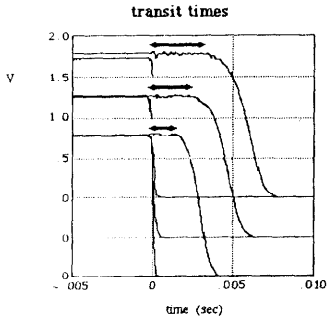

Fig. 11. Evaluation of transit times from raw data in three different gap sizes. The drop in the voltage vs. time diagrams shows the motion of outer and inner cylinder for the 12.2 mm gap (top) ($c = 431 \pm 11$ cm s^{-1}), for the 9.38 mm gap (middle) ($c = 403 \pm 34$ cm s^{-1}) and for the 6.12 mm gap (bottom) ($c = 378 \pm 12$ cm s^{-1}). The lengths of the arrows represent the lapse time between the onset of motion of both cylinders in each gap size.

inner cylinder which results from the arriving shear wave. How the transit time is evaluated from graphs of this kind is indicated through the arrows above each pair of signals. The lengths of the arrows represent the elapsed time between the instances of onset of motion of the outer and inner cylinder. Figure 11 shows the development of the transit time over three gap sizes. From here and from Table 5 the reader can verify how well the data satisfy the criterion for the definition of a shear-wave speed given above.

The value $\bar{c}$ was subsequently used to evaluate the delayed die-swell experiments which are discussed in Section 7. We call the flow "sub-" or "supercritical" whenever the local velocity is smaller or larger than the wave speed $\bar{c}$ that was measured on the wave-speed meter.

In order to make a comparison with other fluids tested in our meter we use quantities that can be calculated from the shear-wave speed $\bar{c}$. These are the effective rigidity, $G_c = \rho \bar{c}^2$, where ρ is the density, and the effective relaxation time, $\lambda_c = \tilde{\mu}/G_c$, where $\tilde{\mu}$ is the zero-shear viscosity that was determined from measurements on a Rheometrics System Four rheometer. We believe that $\bar{c}$, G_c and λ_c are relevant for the dynamic properties of flow and for steady flows which change type. G_c represents slowly decaying elastic modes that characterize wave propagation on the time scale of the instrument ($O(10^{-3}$–10^{-4} s)). λ_c is an important estimate for the decay time of these modes.

A comparison with other liquids that have been tested on the wave-speed meter is especially useful (see Riccius [21] for a complete list of wave-speed data obtained until February 1989). The signals were not noisy, facilitating unambiguous evaluation of transit times. We can say that M1 supports wave

propagation over a large distance at high wave speeds relative to most other fluids. In comparison with fluids of similar zero-shear viscosity the large wave speed gives rise to a large effective rigidity G_c and to a rather short effective relaxation time λ_c. The relaxation time is the most significant quantity for this comparison. It effectively reveals whether the liquid has a relatively elastic or Newtonian response. λ_c plays a role in the interpretation of the results on delayed die swell (see Section 7).

7. Delayed die swell

Joseph et al. [22] showed that there is a critical speed of extrusion beyond which the swell is delayed; instead of swelling at the exit lip, as it does in the pre-critical case, the extrudate does not swell at the exit but the swell begins somewhat farther downstream. Many photographs are shown in their paper.

A sketch of delayed die swell in fluids with a relatively long time of relaxation, say $\lambda_c > 10^{-2}$ s, is shown in Fig. 12.

Joseph et al. [22] found that the shape of the jet appears to correlate with the time of relaxation based on our wave speed which was discussed in Section 6. The fluids with long times of relaxation are more elastic, and the delay is very pronounced, like a hydraulic jump, as in Fig. 12. Fluids with short times of relaxation are more Newtonian with larger effective viscosities, smoothing shocks. We think of Jeffreys' model with large Newtonian viscosities, large retardation times. For these fluids it is much harder to detect the delay. The delay appears as a change of curvature, a point of inflection in the jet shape which is introduced at criticality.

In Fig. 13 we exhibit a sequence of photographs which shows how the shape of the jet of M1 changes as the speed of extrusion is increased past criticality. The extrusion velocity $\bar{u}$ is the volume flow rate divided by the area of the pipe. Ahrens et al. [23] have shown that vorticity of the Poiseuille

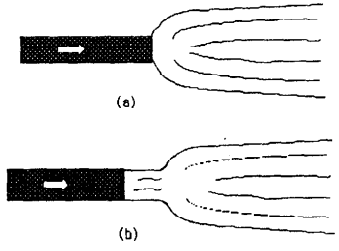

Fig. 12. Sketch of delayed die swell in a solution with a not-too-short time of relaxation: (a) subcritical, (b) supercritical. The speed is greater than the wave speed before the swell, less than the wave speed after the swell.

flow of an upper-convected Maxwell model changes type when the maximum speed u_m at the center of the pipe exceeds the wave speed c. Since $u_m = 2\bar{u}$ for the Maxwell fluid, theory shows that a hyperbolic region appears in the center of the pipe when

$$M = u_m/c = 2\bar{u}/c > 1. \tag{7.1}$$

The procedures used to obtain the values of $\bar{u}$ and c are exactly the same as those described by Joseph et al. [22]. Photograph 13(a) shows a subcritical

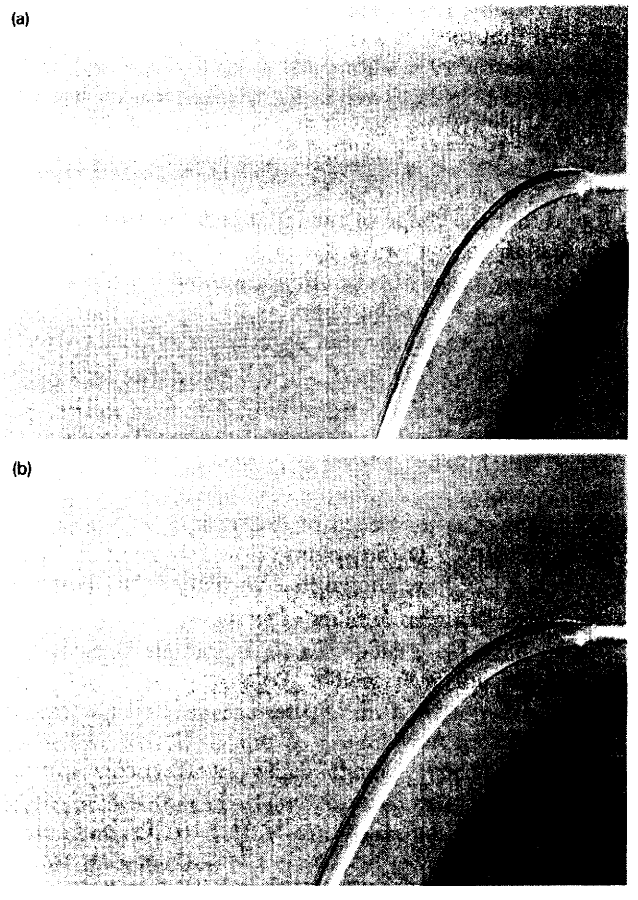

Fig. 13. Delayed die swell of M1. The inside diameter of the pipe is 3.175 mm. (a) $\bar{u} = 312.88$ cm s^{-1}, $M = 2\bar{u}/c = 1.55$, subcritical. (b) $\bar{u} = 357.58$ cm s^{-1}, $M = 1.77$, critical. (c) $\bar{u} = 417.17$ cm s^{-1}, $M = 2.06$, supercritical. (d) $\bar{u} = 500.60$ cm s^{-1}, $M = 2.47$, supercritical.

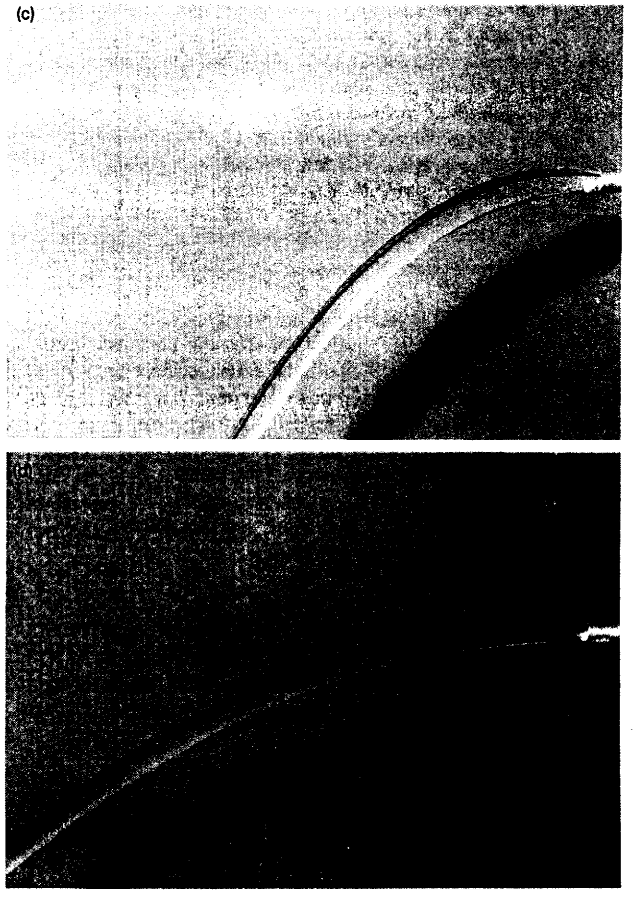

swell; the curvature of the jet is one signed. Photograph 13(b) shows the condition of the jet slightly after criticality. A point of inflection in the curvature appears at the exit lip. We can see this on the videotapes of our experiments, which are available on request, as a sort of sudden stiffening of the jet. Photographs 13(c) and 13(d) show the jet under supercritical conditions. We did measurements and found delays in pipes with different diameters.

The critical conditions for delay in the different pipes are the set of points belonging to M1 shown in Fig. 14.

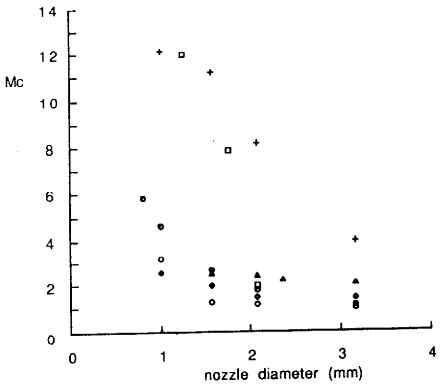

Fig. 14. Mach number vs. pipe diameter: ○, 1.3% CMC; □, 9.8% Elvacite; ◇, 6% PIB/D; ⊖, 2.5% Polyox; +, 12.1% K-125; △, M1.

We found that the shapes of jets of M1 were essentially identical with shapes in other fluids with short times $\lambda = \tilde{\mu}/G_c$ of relaxation. The effective time of relaxation for M1 is 0.00021 s. We refer the reader to Figs. 8.1 and 8.2 of the paper by Joseph et al. [22]. The effective time of relaxation for PIBM, 1%, and PMMA, 1%, are listed in Table 1 of Ref. 22 as 0.0020 s and 0.0059 s respectively, one order greater than the 2.6×10^{-4} s for M1. The jets shown in Joseph et al. [22] were extruded downward, in the direction of gravity, while those shown in Fig. 13 are extruded perpendicular to gravity. The effect of gravity in the vertical jet is to accelerate the jet, to stretch it and to conceal features which might be better seen in a horizontal jet. A PIBM, 1%, jet extruded horizontally would probably look much like M1.

M1 seems to be close to a Newtonian fluid with small non-Newtonian effects which are often associated with highly viscous liquids.

Acknowledgements

This work was supported by the Army Research Office and the National Science Foundation.

References

1 D.D. Joseph, G.S. Beavers, A. Cers, C. Dewald, A. Hoger and P. Than, Climbing constants for various liquids, J. Rheol., 28 (1984) 325–384.
2 D.D. Joseph, Remarks on inertial radii, persistent normal stresses, secondary motions and non-elastic extensional viscosity, J. Non-Newtonian Fluid Mech., 32 (1) (1989).
3 A. Kaye, The shape of a liquid surface between rotating concentric cylinders, Rheol. Acta, 12 (1972) 207–221.

4 D.D. Joseph and R. Fosdick, The free surface on a liquid between cylinders rotating at different speeds, part I, Arch. Ration. Mech. Anal., 49 (1973) 321–380.
5 A.H. Hoffman and W.G. Gottenberg, Determination of the materials functions from a study of the climbing effect, Trans. Soc. Rheol., 17 (1973) 465–485.
6 G. Böhme, Eine Theorie für sekundäre Stromungserscheinungen in nicht-Newtonschen Fluiden, Dtsch. Luft- Raumfahrt, Forschungsber., (1974) 74–84.
7 D.D. Joseph, G.S. Beavers and R. Fosdick, The free surface on a liquid between cylinders rotating at different speeds, part II, Arch. Ration. Mech. Anal., 49 (1973) 381–401.
8 G.S. Beavers and D.D. Joseph, The rotating rod viscometer, J. Fluid Mech., 69 (1975) 475–511.
9 R. Roscoe, The steady elongation of elasto-viscous liquid, Br. J. Appl. Phys., 16 (1965) 1567–1571.
10 S. Zahorski, Flows with constant stretch history and extensional viscosity, Arch. Mech. Stosow., 23 (1971) 433–445.
11 R. Tanner, Engineering Rheology, Clarendon, Oxford, 1985.
12 D.D. Joseph, Stability of Fluid Motions, Springer, Berlin, 1976.
13 D.D. Joseph and G.S. Beavers, Free surface problems in rheological fluid mechanics, Rheol. Acta, 16 (1977) 69–89.
14 K. Walters, The second-normal-stress difference project, Reprinted from IUPAC Macro 83, Bucharest, Romania, Plenary and Invited Lectures Part 2, 1983, pp. 227–237.
15 D.M. Binding, D.M. Jones and K. Walters, The shear and extensional flow properties of M1, J. Non-Newtonian Fluid Mech., 35 (1990) 121–135.
16 R.K. Prud'homme, personal communication, 1989.
17 K.J. Mikkelsen, C.W. Macosko and G. Fuller, Opposed jets: an extensional rheometer for low viscosity liquids, XIth Int. Congress on Rheology, Sydney, 1988.
18 P.R. Schunk, J.M. De Santos, C.W. Macosko and L.E. Scriven, Newtonian flow in opposed nozzle configurations, XIth Int. Congress on Rheology, Sydney, 1988.
19 D.D. Joseph, A. Narain and O. Riccius, Shear-wave speeds and elastic moduli for different liquids. Part I. Theory, J. Fluid Mech., 171 (1986) 289–308.
20 D.D. Joseph, O. Riccius and M. Arney, Shear-wave speeds and elastic moduli for different liquids. Part II. Experiments, J. Fluid Mech., 171 (1986) 309–338.
21 O. Riccius, Shear-wave speeds and elastic moduli for different liquids and related topics, Ph.D. Thesis, University of Minnesota, 1989.
22 D.D. Joseph, J. Matta and K. Chen, Delayed die swell, J. Non-Newtonian Fluid Mech., 29 (1987) 31–65.
23 M. Ahrens, J.Y. Yoo and D.D. Joseph, Hyperbolicity and change of type in the flow of viscoelastic fluids through pipes, J. Non-Newtonian Fluid Mech., 24 (1987) 67–83.